Indian J Pure Appl Math (2026) 57:679–691
https://doi.org/10.1007/s13226-024-00728-8

ORIGINAL RESEARCH

Collision between weak shock waves for a two-layer blood flow model

M. Manikandan · M. Venkateshprasath · Sahadeb Kuila · T. Raja Sekhar

Received: 13 May 2024 / Accepted: 25 November 2024 / Published online: 20 December 2024

Abstract This paper investigates the collision of two weak shocks of the Riemann problem for a two-layer blood flow model characterized by physiological parameter representative of arteries. The model considered vertical averages across each layer derived from the Euler equations of gas dynamics, which described a quasi-linear hyperbolic system of conservation laws. We explore the elementary waves, specifically the shock, rarefaction and contact discontinuity, using the method of characteristics and derive the curves in one parameter form. Moreover, the existence-uniqueness of the Riemann solution is proved locally, ensuring its compatibility with numerical simulations, for arbitrary data. Furthermore, we determine a necessary and sufficient condition for shock waves or rarefaction waves based on the initial data of the Riemann problem. At the end, the interaction of two weak shocks from the same family is analyzed explicitly.

Keywords Blood flow model · Riemann problem · Existence and uniqueness · Weak shock · Wave interaction

1 Introduction

The blood flow model played a crucial role in the study of larger vessels such as arteries and veins. The fluid transfer in flexible tubes that characterizes blood flow through arterial circulation may be theoretically modeled using the conservation of mass and momentum. The Riemann problem studies in blood flow models gained significant attention, from both a physical and mathematical perspective, as a result of their application in various fields, including engineering, clinical practice, medical research and fluid dynamics, among others. For more information, refer to [1–4]. This model greatly contributed to our understanding of cardiovascular health, medical interventions and fluid dynamics analysis. The history of arterial wave mechanics was briefly discussed in [5]. Euler [6] developed a model using a distensible tube to describe blood circulation in arteries while setting out the one-dimensional equations of conservation of mass and momentum. Nevertheless, he could have ascertained the waves nature, hindering the formulation of a definitive solution. Euler's conservation equations were rediscovered in their linearized form by Wilhelm [7] over a century later. Despite later creating multidimensional blood flow models, the one-dimensional model was more straightforward and easier to use. Various techniques were employed to establish a numerical solution for the one-dimensional blood flow model,

Communicated by G.D. Veerappa Gowda.

M. Manikandan · M. Venkateshprasath · S. Kuila
Department of Mathematics, SRM Institute of Science and Technology, Kattankulathur, Tamil Nadu 603203, India
E-mail: sahadebk@srmist.edu.in, sahadebkuila@gmail.com

T. Raja Sekhar (✉)
Department of Mathematics, Indian Institute of Technology Kharagpur, Kharagpur 721302, India
E-mail: trajasekhar@maths.iitkgp.ernet.in

including ADER finite volume scheme [8], the formulation of exactly balanced solvers [9] and a fully well-balanced scheme [10]. Some researchers studied different mathematical models to explore the various aspects of blood flow in stenotic arteries by representing blood as a single-layer model. Several studies in [11–13] investigated blood flow between the two layers of a stenotic tube.

A two-layer blood flow model characterized by distinct velocities while maintaining constant densities within each layer was considered by Zhang et al. [14] as

$$\partial_t A_1 + \partial_x(A_1 u_1) = M_{in}, \tag{1.1a}$$

$$\partial_t(A_1 u_1) + \partial_x(A_1 u_1^2) + \frac{A_1}{\rho_1}\partial_x p_1 = U_{in} M_{in}, \tag{1.1b}$$

$$\partial_t A_2 + \partial_x(A_2 u_2) = -M_{in}, \tag{1.1c}$$

$$\partial_t(A_2 u_2) + \partial_x(A_2 u_2^2) + \frac{A_2}{\rho_2}\partial_x p_2 = -U_{in} M_{in}. \tag{1.1d}$$

In this context, A_i, u_i, ρ_i and p_i (where $i = 1, 2$) corresponded to the characteristics of the i^{th} layer of blood flow within a vessel. Here, A_i denotes the cross-sectional area at a given location (x) and time (t), u_i represents the horizontally averaged speed and ρ_i the density of blood in the same layer. Additionally, M_{in} indicates the mass that is exchanged from the second layer to the first layer and U_{in} denotes the free interface velocity between every layer, which is left to be specified. Lastly, the pressure p_i in the i-th layer is related to the cross-sectional area $A(x, t)$ by the algebraic relation of the form [14]

$$p_i(x,t) = k(x)\left[\left(\frac{A_i(x,t)}{A_e(x)}\right)^m - \left(\frac{A_i(x,t)}{A_e(x)}\right)^n\right].$$

The elastic characteristics of the vessel are described by the constant coefficient $k(x)$ [15,16]

$$k(x) = \frac{\sqrt{\pi}\, h_e(x)\mathcal{E}(x)}{(1-\nu^2)\sqrt{A_e(x)}}$$

is derived from the relationship involving the Poisson ratio ν, the wall thickness of the vessel denoted as $h_e(x)$, Young's modulus represented as $\mathcal{E}(x)$, along with the cross-sectional area in its equilibrium state denoted by $A_e(x)$. In the past, the parameters $m \geq 0$ and $n \leq 0$ were established through empirical observations or derived from higher-order models [17]. This study explores the blood flow in arteries, where $m = \frac{1}{2}$ and $n = 0$. The original model (1.1) contains the viscous terms but it is a non-conservative form. Additionally, this system exhibits conditional hyperbolicity and its eigenstructure avoids explicit determination. However, it should be noted that the existing literature is very limited. In view of these difficulties, the researchers [14,18–20] made some assumptions and manipulations that the two layers are homogeneous, with the consistent cross-sectional area and free interface velocity

$$\rho_1 = \rho_2 = \rho,\ A_1 = A_2 = \frac{1}{2}A,\ \bar{u} = \frac{u_1 + u_2}{2} \text{ and } \hat{u} = \frac{u_2 - u_1}{2} \tag{1.2}$$

to simplify the governing two-layer model into a conservative form. Here, $\bar{u}$ and $\hat{u}$ are represented as the horizontal blood flow velocities, with $\bar{u}$ being denoted as the vertical average and $\hat{u}$ being indicated as the oriented standard deviation. This distinction is a fundamental departure from the single-layer model, which incorporated just one degree of freedom for velocity [14]. Moreover, this comparable relationship (1.2) was also assumed for the traffic flow model [21] and shallow water model [22]. To obtain the conservative form, subtract the two mass equations mentioned in (1.1),

$$\partial_x(A\hat{u}) = -2M_{in}. \tag{1.3}$$

Repeatedly, using (1.3), (1.1b) subtract from (1.1d), we get

$$\partial_t(A\hat{u}) + \partial_x(2A\bar{u}\hat{u}) = \bar{u}\partial_x(A\hat{u}). \tag{1.4}$$

By utilizing equations (1.1), the concise expression for the two-layer blood flow model as

$$\partial_t A + \partial_x(A\bar{u}) = 0, \tag{1.5a}$$

$$\partial_t(A\bar{u}) + \partial_x\left(A(\bar{u}^2 + \hat{u}^2) + \frac{mk}{\rho(m+1)}\frac{A^{m+1}}{A_e^m}\right) = 0. \tag{1.5b}$$

The third equation could be derived by using (1.4) into (1.5), we have

$$\partial_t\hat{u} + \partial_x(\hat{u}\bar{u}) = 0. \tag{1.6}$$

Equations (1.5) and (1.6) represent an equivalent conservative model to the two-layer blood flow model (1.1). Since the simplified two layer model is in conservative form and strictly hyperbolic so it admits shock waves.

The investigation of the Riemann problem in the context of a two-layer blood flow model is fascinating, with significant relevance from both mathematical and physical perspectives. The Riemann problem initiated by Riemann [23] is a classical problem with the study of hyperbolic conservation laws. Lax [24] solved the Riemann problem when initial data consisting of constant states $\mathfrak{I}_l$ and $\mathfrak{I}_r$ are sufficiently close to one another. Smoller [25] analyzed the collision of the one-dimensional elementary waves in gas dynamics of the Riemann problem. For a good source of Riemann solutions, see [26–30]. The precise structure of the Riemann solution in a non-ideal gas dynamics model and the collision of weak shocks were discussed by Ambika and Radha [31]. Pandey and Sharma [32] investigated the collision of a characteristic shock with a weak discontinuity in a non-ideal gas. Wave collisions of the Riemann problem for various physical models were discussed in [33–35].

In this study, our primary goal is to explore the collision of weak shocks of the Riemann solution for the two-layer blood flow model in arteries, where velocities vary and the density remains constant within every layer. The new model accounted for both the standard deviation of two-layer speeds as well as the average blood flow rate. Here, we derive the one-parameter families of curves for shock waves, rarefaction waves, and contact discontinuity regarding blood flow parameters. The existence and uniqueness of the Riemann solution are proved, ensuring its compatibility with numerical simulations, for arbitrary initial data. An algorithm is developed to assess whether the solution's 1 or 3-component is a shock or a rarefaction wave regarding initial data. Additionally, von Neumann's [36] finding on the collision of weak shock waves from the same family is examined. This discovery, in our opinion, contributes significantly to our understanding of the wave dynamics in blood flow via two-layered arteries and advances mathematical biology theory as well as its many real-world applications in science and engineering.

This paper is organized as follows: In Sect. 2, the Riemann problem of the one-dimensional two-layer blood flow model is considered in a conservative form and explores its characteristics analysis. The Riemann problem's elementary waves are briefly discussed in Sect. 3. In Sect. 4, families of Riemann solutions dependent on a single parameter are explored. The existence and uniqueness of the solution to the Riemann problem and possible occurrences of shocks or simple waves in one and three-family waves are proved in Sect. 5. Section 6 analyzes the collision of two weak shocks from the same family. A conclusion and future research regarding the entire study are presented in Sect. 7.

2 Conservative formulation of the Riemann problem

One-dimensional homogeneous blood flow in arteries is governed by the two-layer blood flow model (1.5) and (1.6) takes the conservative form

$$\partial_t \mathrm{V} + \partial_x F(\mathrm{V}) = 0, t \in \mathbb{R}^+, x \in \mathbb{R}, \tag{2.1}$$

where V and F represent vectors of conserve quantities and fluxes, respectively, $\mathrm{V} = \begin{pmatrix} A \\ A\bar{u} \\ \hat{u} \end{pmatrix}$, $F(\mathrm{V}) = \begin{pmatrix} A\bar{u} \\ A(\bar{u}^2 + \hat{u}^2) + \frac{mk}{\rho(m+1)}\frac{A^{m+1}}{A_e^m} \\ \hat{u}\bar{u} \end{pmatrix}$. The Riemann problem for the system (2.1) is characterized by the piecewise constant initial data exhibiting a single discontinuity at the origin

$$\mathfrak{I}(x,0) = \begin{cases} \mathfrak{I}_l \equiv (A_l, \bar{u}_l, \hat{u}_l)^T, & x < 0, \\ \mathfrak{I}_r \equiv (A_r, \bar{u}_r, \hat{u}_r)^T, & x > 0, \end{cases} \tag{2.2}$$

where $\mathfrak{I}_l$ and $\mathfrak{I}_r$ two prescribed constant vectors with $\mathfrak{I} = (A, \bar{u}, \hat{u})^T$ is primitive variable or physical variable.

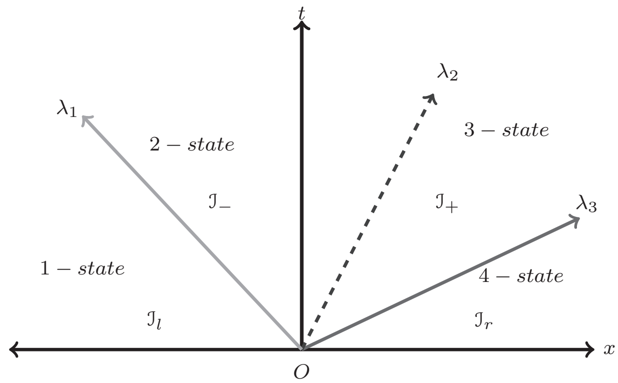

Fig. 1 Elementary waves structure of the Riemann problem for two-layer blood flow model

2.1 Characteristic fields

To consider a smooth solution, the system (2.1) can be expressed in a non-conservative form, which is equivalent to

$$\partial_t \mathcal{I} + M(\mathcal{I})\partial_x \mathcal{I} = 0, \tag{2.3}$$

having the Jacobian matrix $M(\mathcal{I}) = \begin{pmatrix} \bar{u} & A & 0 \\ \hat{u}^2 + \frac{mk}{\rho}\left(\frac{A}{A_e}\right)^m & A\bar{u} & 2A\hat{u} \\ 0 & \hat{u} & \bar{u} \end{pmatrix}$. The eigenvalues of the Jacobian matrix $M(\mathcal{I})$ are $\lambda_1 = \bar{u} - w,\ \lambda_2 = \bar{u}$ and $\lambda_3 = \bar{u} + w$, $w = \sqrt{3\hat{u}^2 + \frac{mk}{\rho}\left(\frac{A}{A_e}\right)^m} > 0$. Furthermore, the corresponding right eigenvectors are given by $\Gamma_1 = (A, -w, \hat{u})^T$, $\Gamma_2 = \left(2A\hat{u}, 0, -\hat{u}^2 - \frac{mk}{\rho}\left(\frac{A}{A_e}\right)^m\right)^T$, $\Gamma_3 = (A, w, \hat{u})^T$.

Because the 3×3 matrix M has three real and distinct eigenvalues, the system (2.1) is strictly hyperbolic. Now, for $j = 1, 3$ and $\nabla \equiv \left(\frac{\partial}{\partial A}, \frac{\partial}{\partial \bar{u}}, \frac{\partial}{\partial \hat{u}}\right)$, we explore

$$\begin{aligned} \nabla\lambda_j.\Gamma_{(j)} &= \pm\left[-2w + \frac{m(2-m)k}{2\rho w}\left(\frac{A}{A_e}\right)^m\right] \\ &= \pm\frac{1}{w}\left[-2w^2 + \frac{m(2-m)k}{2\rho}\left(\frac{A}{A_e}\right)^m\right] \\ &= \pm\frac{1}{w}\left[-6\hat{u}^2 - (1+m)\frac{mk}{\rho}\left(\frac{A}{A_e}\right)^m\right] \\ &\neq 0, \end{aligned}$$

for any values of $w = \sqrt{3\hat{u}^2 + \frac{mk}{\rho}\left(\frac{A}{A_e}\right)^m} > 0$, where $\rho > 0, k > 0, A_e > 0$ and $m = 0.5$ in arteries. Since the quantity is non-zero, it can be concluded that both of the characteristic fields are genuinely nonlinear. Hence, the wave associated with the first or third characteristic field can be either a shock or a rarefaction wave. Again, we get $\nabla\lambda_2.\Gamma_2 = 0$. So the second characteristic field is linearly degenerate. It is composed of contact discontinuity.

3 Elementary waves

Let $\mathcal{I}_l$, $\mathcal{I}_- = (A_-, \bar{u}_-, \hat{u}_-)^T$, $\mathcal{I}_+ = (A_+, \bar{u}_+, \hat{u}_+)^T$ and $\mathcal{I}_r$ are constant states of the entire region divided by three elementary waves as illustrated in Fig. 1.

3.1 Discontinuous waves

The solution along discontinuities for system (2.1) fulfills the Rankine-Hugoniot (R-H) jump condition, where the speed of the discontinuous wave is represented as **s**, leading to the subsequent expression:

$$\begin{aligned}
&-\mathbf{s}[A] + [A\bar{u}] = 0, \\
&-\mathbf{s}[A\bar{u}] + \left[A(\bar{u}^2 + \hat{u}^2) + \frac{mk}{\rho(m+1)}\frac{A^{m+1}}{A_e^m}\right] = 0, \\
&-\mathbf{s}[\hat{u}] + [\bar{u}\hat{u}] = 0.
\end{aligned} \tag{3.1}$$

The expression [.] denotes the jump across the wave as $[\mathcal{J}] = \mathcal{J}_+ - \mathcal{J}_-$. Continuing the computation of (3.1), it becomes evident that this discontinuity can be categorized into two distinct kinds.

1. Contact discontinuity wave: The wave with a speed $\mathbf{s}_2$ satisfying the parallel characteristic condition and R-H conditions (3.1). From (3.1), we get

$$J : \mathbf{s}_2 = \bar{u}, [\bar{u}] \equiv \left[A\hat{u}^2 + \frac{mk}{\rho(m+1)}\frac{A^{m+1}}{A_e^m}\right] = 0. \tag{3.2}$$

   So, along the contact discontinuity curve J, $\bar{u}$ and $A\hat{u}^2 + \frac{mk}{\rho(m+1)}\frac{A^{m+1}}{A_e^m}$ (which is treated like $\mathcal{P}$) stay the same. When they are projected onto the $(A, \bar{u})$-plane, they make a straight line that is parallel to the A-axis in the space (A,$\bar{u}$,$\hat{u}$).
   The Euler equation pressure is comparable to $\mathcal{P}$, but it also takes into consideration the shear effect, which is reflected in $\mathcal{P}$.
2. Shock waves (1-shock ($\mathcal{S}_1$) with speed $\mathbf{s}_1$ or 3-shock ($\mathcal{S}_3$) with speed $\mathbf{s}_3$):
   By using R-H conditions (3.1) with Lax entropy conditions, we obtain 1 and 3-shock wave curves as

$$\mathcal{S}_1(A, \mathcal{J}_l) : \begin{cases} \bar{u} = \bar{u}_l - w_l\sqrt{\dfrac{\left(\left(\frac{A_l}{A}\right)-1\right)\left[\left(1-\left(\frac{A}{A_l}\right)^3\right)+\frac{\delta}{m+1}\left(1-\left(\frac{A}{A_l}\right)^{m+1}\right)\right]}{3+\delta}}, \\ \hat{u} = \beta_l A, \end{cases} \tag{3.3}$$

   and

$$\mathcal{S}_3(A, \mathcal{J}_r) : \begin{cases} \bar{u} = \bar{u}_r + w_r\sqrt{\dfrac{\left(\left(\frac{A_r}{A}\right)-1\right)\left[\left(1-\left(\frac{A}{A_r}\right)^3\right)+\frac{\delta'}{m+1}\left(1-\left(\frac{A}{A_r}\right)^{m+1}\right)\right]}{3+\delta'}}, \\ \hat{u} = \beta_l A, \end{cases} \tag{3.4}$$

   where $\delta = \frac{mk}{\rho\hat{u}_l^2}\left(\frac{A_l}{A_e}\right)^m$ and $\delta' = \frac{mk}{\rho\hat{u}_r^2}\left(\frac{A_r}{A_e}\right)^m$. Also, we explore that $A_l < A, \bar{u}_l > \bar{u}, \hat{u}_l < \hat{u}$ for $\mathcal{S}_1$ and $A > A_r, \bar{u} > \bar{u}_r, \hat{u} > \hat{u}_r$ for $\mathcal{S}_3$.

3.2 Rarefaction waves

Consider that the one and three-characteristic fields display 1-rarefaction wave ($\mathcal{R}_1$) or 3-rarefaction wave ($\mathcal{R}_3$). To identify all rarefaction wave solutions of the system (2.1), let $A = A_1(\tau)$, $\bar{u} = U_1(\tau)$, and $\hat{u} = U_2(\tau)$, where A, $\bar{u}$, and $\hat{u}$ are functions of τ, which themselves are dependent on the independent variables x and t. Subsequently, the system (2.1) simplifies to

$$\begin{aligned}
&\frac{dA_1}{d\tau}\left(\frac{\partial\tau}{\partial t} + U_1\frac{\partial\tau}{\partial x}\right) + A_1\frac{dU_1}{d\tau}\frac{\partial\tau}{\partial x} = 0, \\
&\frac{dU_2}{d\tau}\left(\frac{\partial\tau}{\partial t} + U_1\frac{\partial\tau}{\partial x}\right) + U_2\frac{dU_1}{d\tau}\frac{\partial\tau}{\partial x} = 0, \\
&\frac{dU_1}{d\tau}\left(\frac{\partial\tau}{\partial t} + U_1\frac{\partial\tau}{\partial x}\right) + \left[\left(\frac{3U_2^2}{A_1}\frac{mk}{\rho}\frac{A_1^{m-1}}{A_e^m}\right)\frac{dA_1}{d\tau}\right]\frac{\partial\tau}{\partial x} = 0.
\end{aligned} \tag{3.5}$$

If $\frac{dA_1}{d\tau}$ is nonzero, the system can be expressed as follows

$$\left(-A_1\frac{dU_2}{d\tau}\frac{dU_1}{d\tau}+U_2\frac{dA_1}{d\tau}\frac{dU_1}{d\tau}\right)\frac{\partial\tau}{\partial x}=0, \tag{3.6}$$

$$\left(-A_1\frac{dU_1}{d\tau}\frac{d\tau}{dt}+U_1\frac{dU_1}{d\tau}+\left(\frac{3U_2^2}{A_1}\frac{mk}{\rho}\frac{A_1^{m-1}}{A_e^m}\right)\frac{dU_1}{d\tau}\right)\frac{\partial\tau}{\partial x}=0.$$

which leads to

$$\frac{dU_2}{d\tau}=\frac{U_2}{A_1}\frac{dA_1}{d\tau}, \tag{3.7}$$

$$\left(\frac{dU_2}{d\tau}\right)^2=\left(\frac{3U_2^2}{A_1^2}+\frac{mk}{\rho}\frac{A_1^{m-2}}{A_e^m}\right)\left(\frac{dA_1}{d\tau}\right)^2,$$

or

$$\frac{dU_1}{d\tau}=\frac{dU_2}{d\tau}=0. \tag{3.8}$$

Without loss of generality, one can choose $A_1(\tau)=\tau$ by solving the equations (3.7), we get

$$\bar{u}=U_1(A)=c_1\pm\int\sqrt{3c_1^2+\frac{mk}{\rho}\frac{A^{m-2}}{A_e^m}}dA,$$

$$\hat{u}=U_2(A)=Ac_2,$$

It is observed that $\frac{U_2(A)}{A}$, $\bar{u}+U_1(A)$ (respectively, $\bar{u}-U_1(A)$) are the invariant solutions, *i.e.*, constant solutions of the system (2.1) along the characteristics $\frac{dx}{dt}=\lambda_1$ (respectively, λ_3). In view of $\bar{u}_l=U_1(A_l)$ and $\hat{u}_l=U_2(A_l)$, the $\mathcal{R}_1$ solution can be written as

$$\mathcal{R}_1(A,\mathcal{I}_l):\begin{cases}\bar{u}=\bar{u}_l+\frac{2w_l}{m}\left(\sqrt{\frac{3\left(\frac{\hat{u}_l}{A_l}\right)^2A^2+\frac{mk}{\rho}\left(\frac{A}{A_e}\right)^m}{3\hat{u}_l^2+\frac{mk}{\rho}\left(\frac{A_l}{A_e}\right)^m}}-1\right),\\ \hat{u}=\left(\frac{\hat{u}_l}{A_l}\right)A.\end{cases} \tag{3.9}$$

Similarly, it can be established for $\mathcal{R}_3$,

$$\mathcal{R}_3(A,\mathcal{I}_r):\begin{cases}\bar{u}=\bar{u}_r-\frac{2w_r}{m}\left(\sqrt{\frac{3\left(\frac{\hat{u}_r}{A_r}\right)^2A^2+\frac{mk}{\rho}\left(\frac{A}{A_e}\right)^m}{3\hat{u}_r^2+\frac{mk}{\rho}\left(\frac{A_r}{A_e}\right)^m}}-1\right),\\ \hat{u}=\left(\frac{\hat{u}_r}{A_r}\right)A.\end{cases} \tag{3.10}$$

In the context of rarefaction waves, it's observed that the characteristic speed increases as we move from left to right. This implies that $A_l\geq A$, $\bar{u}_l\leq\bar{u}$, $\hat{u}_l\geq\hat{u}$ for $\mathcal{R}_1$ and $A\leq A_r$, $\bar{u}\leq\bar{u}_r$, $\hat{u}\leq\hat{u}_r$ for $\mathcal{R}_3$.

4 One-parameter families of curves

To make the construction of the elementary waves of the Riemann problem (2.1) and (2.2) further explicit, bring in a new variable, represented by z, defined as $z=-\log\left(\frac{A}{A_l}\right)$. Therefore, based on equations (3.3) and (3.9) for shock and rarefaction wave in one-family, respectively, we obtain $\frac{A}{A_l}=e^{-z}$. Now, we can conclude that $\mathcal{S}_1$ have $z<0$ and $\mathcal{R}_1$ have $z\geq0$. In a similar manner in three-family, we define z as $z=\log\left(\frac{A_r}{A}\right)$. Therefore, by utilizing equations (3.4) and (3.10) for shock and rarefaction wave in three-family, respectively, we find that $\frac{A_r}{A}=e^z$. So, we can infer that z is $z<0$ for $\mathcal{S}_3$ and $z\geq0$ for $\mathcal{R}_3$. In the case of the two-family, we define

$\frac{A}{A_l} = e^{-z}$, where z ranges over the entire real number line: $-\infty < z < \infty$. Hence, we can consolidate our expressions for the one-parameter families of curves for z in the real number set ($z \in \mathbb{R}$) like this.

For *one-family*:

$$
\begin{aligned}
&\frac{A}{A_l} = \Phi_1(z) \equiv e^{-z}, \\
&\frac{\hat{u}}{\hat{u}_l} = e^{-z}, \\
&\frac{\bar{u} - \bar{u}_l}{w_l} = \\
&\psi_1(z) \equiv \begin{cases} -\sqrt{\frac{(e^z-1)[(1-e^{-3z})+\frac{\delta}{m+1}(1-e^{-(m+1)z})]}{3+\delta}}, & z < 0, \\ \frac{2}{m}\left(\sqrt{\frac{3e^{-2z}+\frac{\delta}{m+1}e^{-mz}}{3+\delta}} - 1\right), & z \geq 0, \end{cases}
\end{aligned}
\tag{4.1}
$$

For *two-family*:

$$
\begin{aligned}
&\frac{A}{A_l} = e^{-z}, \\
&\frac{\bar{u}}{\bar{u}_l} = 1, \\
&\frac{\hat{u}}{\hat{u}_l} = e^{2z} + \frac{\delta}{m+1}[e^{2z} - e^{(1-m)z}],
\end{aligned}
\tag{4.2}
$$

For *three-family*:

$$
\begin{aligned}
&\frac{A_r}{A} = \Phi_3(z) \equiv e^{z}, \\
&\frac{\hat{u}_r}{\hat{u}} = e^{z}, \\
&\frac{\bar{u} - \bar{u}_r}{w_r} = \\
&\psi_3(z) \equiv \begin{cases} \sqrt{\frac{(e^z-1)[(1-e^{-3z})+\frac{\delta'}{m+1}(1-e^{-(m+1)z})]}{3+\delta'}}, & z < 0, \\ -\frac{2}{m}\left(\sqrt{\frac{3e^{-2z}+\frac{\delta'}{m+1}e^{-mz}}{3+\delta'}} - 1\right), & z \geq 0. \end{cases}
\end{aligned}
\tag{4.3}
$$

5 Solution strategy

The one-parameter families (4.1)-(4.3) are helpful to represent in general notation, therefore, we define $\mathfrak{I} = (u_1, u_2, u_3)^T \equiv (A, \bar{u}, \hat{u})^T$. We introduce the transformations T_z^q, where $q = 1, 2, 3$. The q-shock wave or q-rarefaction wave for $q = 1, 3$ is connected between its left and right states by these transformations. While for the contact discontinuity, it is linked through T_z^2. Hence we have

$$T_z^1\mathfrak{I} = (\Phi_1(z)u_1, u_2 + w_l\psi_1(z), \Phi_1(z)u_3)^T, \tag{5.1}$$

$$T_z^2\mathfrak{I} = \left(e^{-z}, u_2, e^{2z} + \frac{\delta}{m+1}[e^{2z} - e^{(1-m)z}]u_3\right)^T, \tag{5.2}$$

$$T_z^3\mathfrak{I} = (\Phi_3(z)u_1, u_2 - w_r\psi_3(z), \Phi_3(z)u_3)^T. \tag{5.3}$$

Next, we establish the existence and uniqueness theorem regarding the solution of the Riemann problem.

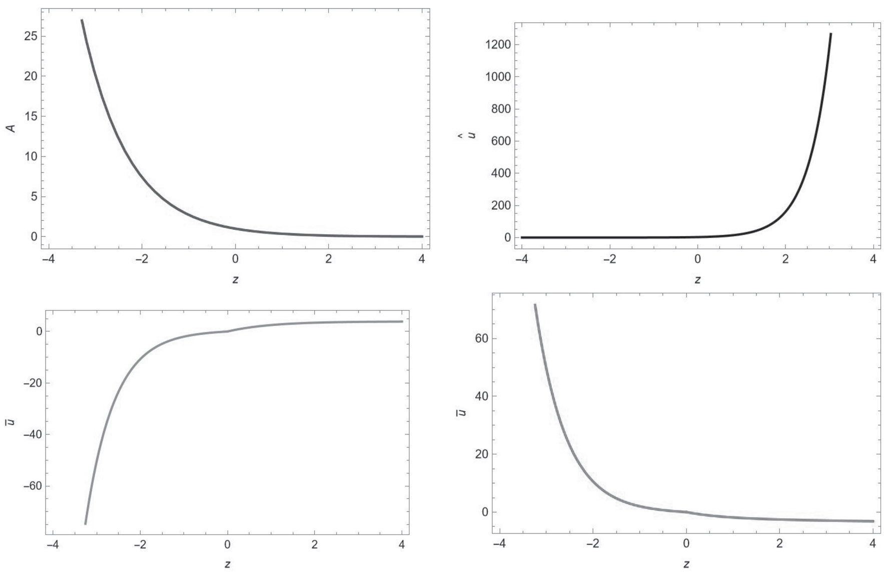

Fig. 2 **a** Cross section-A profile for one-family wave; **b** velocity-$\hat{u}$ profile for two-family wave; **c** velocity-$\bar{u}$ profile for one-family waves **d** velocity-$\bar{u}$ profile for three-family waves

Theorem 5.1 *The Riemann problem solution for the present two-layer blood flow model (2.1) in arteries, given arbitrary initial data (2.2), exists and is unique in the class of solutions consisting of shocks, rarefaction waves and contact discontinues separated by constant states.*

Proof The proof follows based on the ideas of Smoller [25] for the application of gas dynamics. We identify real values z_1, z_2 and z_3 uniquely such that we can solve the Riemann problem (2.1) and (2.2) by

$$\mathcal{I}_r = T^{(3)}_{z_3} T^{(2)}_{z_2} T^{(1)}_{z_1} \mathcal{I}_l, \tag{5.4}$$

i.e.,

$$\begin{pmatrix} A_r \\ \bar{u}_r \\ \hat{u}_r \end{pmatrix} = \begin{pmatrix} \Phi_1(z_1) e^{-z_2} \Phi_3(z_3) A_l \\ \bar{u}_l + w_l \psi_1(z_1, A_l, \hat{u}_l) - w_r \psi_3(z_3, A_r, \hat{u}_r) \\ \Phi_1(z_1)\Phi_3(z_3)\left(e^{2z_2} + \frac{\delta}{m+1}[e^{2z_2} - e^{(1-m)z_2}]\right)\hat{u}_l \end{pmatrix}, \tag{5.5}$$

which follows that

$$\Phi_1(z_1) e^{-z_2} \Phi_3(z_3) = c_1, \tag{5.6}$$

$$w_l \psi_1(z_1, A_l, \hat{u}_l) - w_r \psi_3(z_3, A_r, \hat{u}_r) = c_2, \tag{5.7}$$

$$\Phi_1(z_1)\Phi_3(z_3)\left(e^{2z_2} + \frac{\delta}{m+1}[e^{2z_2} - e^{(1-m)z_2}]\right) = c_3, \tag{5.8}$$

where $c_1 = \frac{A_r}{A_l}$, $c_2 = \bar{u}_r - \bar{u}_l$ and $c_3 = \frac{\hat{u}_r}{\hat{u}_l}$. From (5.6), we obtain

$$z_3 - z_1 - z_2 = \log c_1. \tag{5.9}$$

Using (5.9) in (5.8) yields

$$e^{3z_2}\left(1 + \frac{\delta}{m+1}\left(1 - e^{-(m+1)z_2}\right)\right) = \frac{c_3}{c_1}, \tag{5.10}$$

where $\delta = \frac{mk}{\rho \hat{u}_l^2}\left(\frac{A_l}{A_e}\right)^m$.

Let us define $f(z_2) = (1+\mathcal{A})e^{3z_2} - \mathcal{A}e^{(2-m)z_2} - \mathcal{B}$, where $\mathcal{A} = \frac{mk}{(m+1)\rho\hat{u}_l^2}\left(\frac{A_l}{A_e}\right)^m > 0$ for $m > 0$ and $\mathcal{B} = \frac{A_l \hat{u}_r}{A_r \hat{u}_l} > 0$ and hence, $f'(z_2) = 3(1+\mathcal{A})e^{3z_2} - (2-m)\mathcal{A}e^{(2-m)z_2}$. For $0 < m < 2$, we have $f(z_2)$ is increasing (*i.e.,* $f'(z_2) > 0$) if $z_2 > \frac{1}{m+1}\log\left(\frac{(2-m)\mathcal{A}}{3(1+\mathcal{A})}\right)$ while $f(z_2)$ is decreasing (*i.e.,* $f'(z_2) < 0$) if

$z_2 < \frac{1}{m+1}\log\left(\frac{(2-m)\mathcal{A}}{3(1+\mathcal{A})}\right)$. Since $0 < m < 2$, $f(z_2)$ diverges to ∞ as $z_2 \to \infty$ whilst converges to $-\mathcal{B}$ whenever $z_2 \to -\infty$. Therefore, $f(z_2)$ has a unique solution in $\left(\frac{1}{m+1}\log\left(\frac{(2-m)\mathcal{A}}{3(1+\mathcal{A})}\right), \infty\right)$ for $0 < m < 2$.

In particular, for $m = 0$, $f(z_2) = e^{3z_2} - \mathcal{B}$ and so, $f'(z_2) = 3e^{3z_2} > 0$ for all z_2. Hence, it is obvious that $f(z_2)$ has a unique root in $(-\infty, \infty)$ for $m = 0$.

Therefore, $f(z_2)$ has a unique solution for $0 \leq m < 2$, which includes the blood flow in arteries (*i.e.,* $m = \frac{1}{2}$), say

$$z_2 = a, \tag{5.11}$$

which depends on the constant initial data (2.2). Now, substituting z_2 in (5.9), which yields

$$z_3 = z_1 + a + \log c_1. \tag{5.12}$$

Again, substitute z_3 in (5.7), which yields

$$w_l\psi_1(z_1, A_l, \hat{u}_l) - w_r\psi_3(z_1 + a + \log c_1, A_r, \hat{u}_r) = c_2. \tag{5.13}$$

Let

$$g(z_1) = w_l\psi_1(z_1, A_l, \hat{u}_l) - w_r\psi_3(z_1 + a + \log c_1, A_r, \hat{u}_r) - c_2. \tag{5.14}$$

It is analyzed that $g'(z_1) > 0$ for any values of a. Hence, $g(z_1)$ is a strictly increasing function of z_1. Moreover, $g(z_1)$ diverges to ∞ as $z_1 \to \infty$ and diverges to $-\infty$ as $z_1 \to -\infty$. Hence, there exists a unique solution for $g(z_1)$. So, we calculate uniquely z_1, z_2 and z_3 from (5.14), (5.11) and (5.12), respectively. As a consequence, we obtain a unique solution to the Riemann problem for every pair of initial conditions, denoted as $\mathcal{I}_l$ and $\mathcal{I}_r$. We present a corollary indicating the occurrence of shocks or rarefaction waves in one-family and three-family.

Corollary 5.1 *Consider the solution of the Riemann problem obtained in the above theorem. Then the following statements hold:*

1. $\bar{u}_r - \bar{u}_l < -w_r\psi_3(z_1 + a + \log c_1)$ *iff 1-component of the solution is a shock wave and is a rarefaction wave otherwise.*
2. $\bar{u}_r - \bar{u}_l < -w_l\psi_1(z_3 - a - \log c_1)$ *iff 3-component of the solution is a shock wave and is a rarefaction wave otherwise.*

Proof 1. Let us consider the equation from (5.14) that

$$\mathcal{M}(\zeta) = w_l\psi_1(\zeta) - w_r\psi_3(\zeta + a + \log c_1).$$

Then observe that

$$\mathcal{M}(0) = w_l\psi_1(0) - w_r\psi_3(a + \log c_1) \equiv -w_r\psi_3(a + \log c_1).$$

Again

$$\mathcal{M}'(\zeta) = w_l\psi_1'(\zeta) - w_r\psi_3'(\zeta + a + \log c_1) > 0, \zeta \in \mathbb{R}.$$

Since 1-family of the solution represent a $\mathcal{S}_1$ iff $z < 0$. Hence, for $\mathcal{S}_1$ wave, $\mathcal{M}(z) < \mathcal{M}(0)$, *i.e.*,

$$\bar{u}_r - \bar{u}_l < -w_r\psi_3(z + a + \log c_1).$$

Alternatively, if the subsequent

$$\bar{u}_r - \bar{u}_l < -w_r\psi_3(z + a + \log c_1),$$

holds it can be rewritten as $\mathcal{M}(z) < \mathcal{M}(0)$. Thus, $z < 0$ as $\mathcal{M}$ is a strictly increasing function, *i.e.*, one-family represents a shock wave. Hence, one-family represents a shock wave iff

$$\bar{u}_r - \bar{u}_l < -w_r\psi_3(z + a + \log c_1),$$

Otherwise, it is a $\mathcal{R}_1$.

2. The three-family proof is similar.

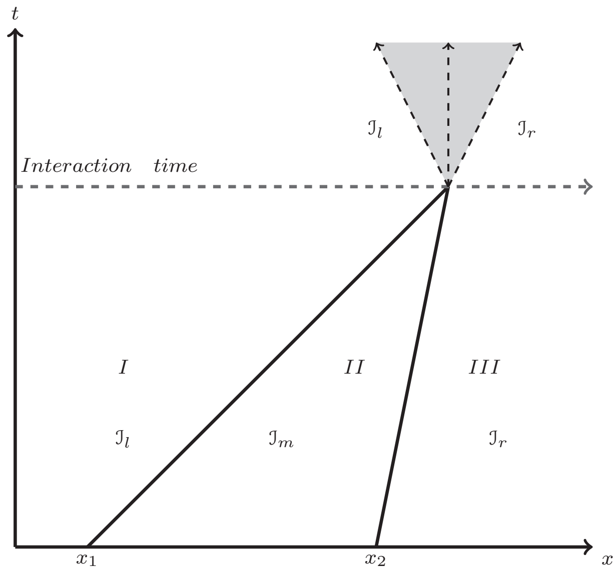

Fig. 3 A collision between two weak $\mathcal{S}_3$ results in a $\mathcal{R}_1$ wave

6 Collision of weak shock waves

We now establish the initial function with two jump discontinuities, located at x_1 and x_2, as follows

$$\mathcal{J}(x,0)=\begin{cases}\mathcal{J}_l, & if \;\; x\leq x_1,\\ \mathcal{J}_m, & if \;\; x_1<x<x_2,\\ \mathcal{J}_r, & if \;\; x\geq x_2.\end{cases} \tag{6.1}$$

by appropriately selecting $\mathcal{J}_m$ and $\mathcal{J}_r$ in relation to $\mathcal{J}_l$ and any arbitrary $x_1, x_2 \in \mathbb{R}$, we can establish two local Riemann problems with the provided initial data (6.1). An elementary wave from the 1-Riemann problem can interact with an elementary wave from the 2-Riemann problem, giving rise to a new Riemann problem at the moment of collision. In this context, we examine the collision of two weak $\mathcal{S}_3$ (or alternatively, $\mathcal{S}_1$) (see, Fig. 3).

Theorem 6.2 *The collision of two weak 3-shocks (respectively, 1-shocks) leads to 1-rarefaction wave (respectively, 3-rarefaction wave).*

Proof We consider that $\mathcal{J}_l=(A_l,\bar{u}_l,\hat{u}_l)^T$ is connected to $\mathcal{J}_m=(A_m,\bar{u}_m,\hat{u}_m)^T$ through $\mathcal{S}_3$ in the 1-Riemann problem, and $\mathcal{J}_m=(A_m,\bar{u}_m,\hat{u}_m)^T$ is connected to $\mathcal{J}_r=(A_r,\bar{u}_r,\hat{u}_r)^T$ via $\mathcal{S}_3$ in the 2-Riemann problem. Thus, the Lax entropy conditions for $\mathcal{S}_3$ in the 1-Riemann problem and 2-Riemann problem are as follows, respectively:

$$\lambda_2(\mathcal{J}_l)<\dot{s}_3<\lambda_3(\mathcal{J}_l),\;\; \lambda_3(\mathcal{J}_m)<\dot{s}_3, \tag{6.2}$$

and

$$\lambda_2(\mathcal{J}_m)<\ddot{s}_3<\lambda_3(\mathcal{J}_m),\;\; \lambda_3(\mathcal{J}_r)<\ddot{s}_3. \tag{6.3}$$

Here, $\dot{s}_3$ and $\ddot{s}_3$ represent the speeds of $\mathcal{S}_3$ in 1-Riemann problem and 2-Riemann problem, respectively. From (6.2) and (6.3), we have $\ddot{s}_3<\dot{s}_3$. Hence, an interaction will occur, and during this interaction, we will be required to solve Riemann problem (2.1) and (2.2), as illustrated in Fig. 3. Using parameters ξ and η, region-I is linked to region-II via $\mathcal{S}_3$ wave in the 1-Riemann problem, while region-II is connected to region-III through $\mathcal{S}_3$ wave in the 2-Riemann problem. Thus, we get

$$\mathcal{J}_m=T_\xi^{(3)}\mathcal{J}_l,\quad \xi<0,\quad \mathcal{J}_r=T_\eta^{(3)}C_m,\quad \eta<0.$$

Hence, the curves (4.3) are as follows

$$A_m=A_le^{\xi},\quad \bar{u}_m=\bar{u}_l-w_m\psi_3(\xi),\quad \hat{u}_m=\hat{u}_le^{\xi}, \tag{6.4}$$

and

$$A_r = A_m e^{\eta}, \quad \bar{u}_m = \bar{u}_r + w_r \psi_3(\eta), \quad \hat{u}_r = \hat{u}_m e^{\eta}. \tag{6.5}$$

Now, we can eliminate $\bar{u}_m$ from (6.4) and (6.5), which yields

$$\bar{u}_l - \bar{u}_r = w_r \left(\frac{w_m}{w_r} \psi_3(\xi) + \psi_3(\eta) \right). \tag{6.6}$$

Contrarily, let's consider that the interaction of two $\mathcal{S}_3$ results $\mathcal{S}_1$, which means that $\bar{u}_r - \bar{u}_l < -w_r \psi_3(y_1 + a + \log \mathcal{J}_1)$ (by using the corollary 5.1), it follows from (6.6) that

$$0 < \left(\frac{\sqrt{3e^{-2\eta}\hat{u}_r^2 + \frac{mk}{\rho}\left(\frac{A_r}{A_e}\right)^m e^{-m\eta}}}{\sqrt{3\hat{u}_r^2 + \frac{mk}{\rho}\left(\frac{A_r}{A_e}\right)^m}} \right) \psi_3(\xi) + \psi_3(\eta) - \psi_3(a + \xi + \eta). \tag{6.7}$$

Let us assume

$$H(\xi, \eta) = \left(\frac{\sqrt{3e^{-2\eta}\hat{u}_r^2 + \frac{mk}{\rho}\left(\frac{A_r}{A_e}\right)^m e^{-m\eta}}}{\sqrt{3\hat{u}_r^2 + \frac{mk}{\rho}\left(\frac{A_r}{A_e}\right)^m}} \right) \psi_3(\xi) + \psi_3(\eta) - \psi_3(a + \xi + \eta).$$

Expanding Taylor's series of H around the origin which yields

$$\begin{aligned}
0 < &\left(\xi + \eta - \frac{1}{2} \left(\frac{6\hat{u}_r^2\rho + \left(\frac{A_r}{A_e}\right)^m m^2 k}{3\hat{u}_r^2\rho + \left(\frac{A_r}{A_e}\right)^m mk} \right) \xi\eta \right.\\
&\left. + \frac{1}{8} \left(\frac{36\hat{u}_r^4\rho^2 + 6\hat{u}_r^2\rho\left(\frac{A_r}{A_e}\right)^m (4 - 2m + m^2)mk + \left(\frac{A_r}{A_e}\right)^{2m} m^3k^2}{\left(3\hat{u}_r^2\rho + \left(\frac{A_r}{A_e}\right)^m mk\right)^2} \right) \xi\eta^2 \right) \psi_3'(0)\\
&- (\xi + \eta)\psi_3'(a) + \frac{1}{2} \left(\xi^2 + \eta^2 - \frac{1}{2} \left(\frac{6\hat{u}_r^2\rho + \left(\frac{A_r}{A_e}\right)^m m^2 k}{3\hat{u}_r^2\rho + \left(\frac{A_r}{A_e}\right)^m mk} \right) \xi^2\eta \right) \psi_3''(0) - \frac{1}{2}(\xi^2 + \eta^2 + 2\xi\eta)\psi_3''(a)\\
&+ \frac{1}{6}(\xi^3 + \eta^3)\psi_3'''(0) - \frac{1}{6}(\xi^3 + \eta^3 + 3\xi^2\eta + 3\xi\eta^2)\psi_3'''(a) + O(\xi^p\eta^q).
\end{aligned} \tag{6.8}$$

Now, substituting the values of $\rho = 1060$, $m = 0.5$, $k = 1000$, $A_e = 3.5$, $A_r = 0.2$, $\hat{u}_r = 30$ [20] in (6.8), we explore

$$0 < -1.033\xi\eta + 1.062\xi^2\eta + 0.545\xi\eta^2 + O(\xi^p\eta^q). \tag{6.9}$$

where $p + q \geq 4$. Since $\xi, \eta < 0$ imply that the right-hand side of inequality (6.9) is negative. Also, it is observed from the Fig. 4. This is leading to a contradiction. Therefore, the collision between two weak $\mathcal{S}_3$ results $\mathcal{R}_1$. Likewise, it can be establish that the collision of two weak $\mathcal{S}_1$ yields $\mathcal{R}_3$.

7 Conclusions

We have considered the Riemann problem of a two-layer blood flow model characterized by physiological parameters representative of arteries, where $m = \frac{1}{2}$ and $n = 0$, with different velocities while keeping density constant. The elementary waves, namely contact discontinuity, rarefaction and shock waves are evaluated by the Rankine-Hugoniot jumps, Lax entropy conditions and their properties. The Riemann solution is explicitly formulated using families of curves parameterized by a single parameter, illustrated in Fig. 2. We have established the existence and uniqueness of the Riemann solution for arbitrary initial data locally. These results are well-suited for compatibility with numerical simulations. An algorithm is developed based on the initial data to determine

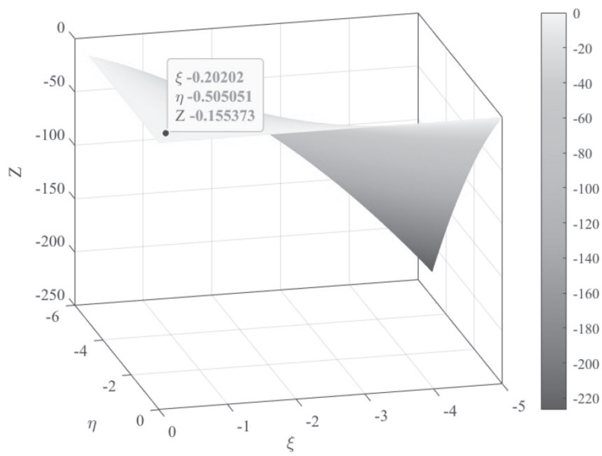

Fig. 4 Graphical representation of the right-hand side of (6.9) for $\xi, \eta < 0$

whether the 1 or 3 components of the solution correspond to a shock or a rarefaction wave. We have discussed the collision of two weak shocks from the same family and it is formed $\mathcal{R}_1$. Our work contributes to advances in mathematical biology theory and its many real-world applications in science and engineering by providing substantial insight into the wave dynamics in blood flow via two-layered arteries.

In the future, the wave interaction between classical elementary waves and delta shock waves of this model will be considered. Also, we will present upwind numerical methods based on the developed exact Riemann solver.

Acknowledgements The first and second authors would like to thank the SRM Institute of Science and Technology, Kattankulathur, Tamil Nadu, India, for their financial support. Research support from SERB, DST, Government of India (Ref. No. CRG/2022/006297) is greatly acknowledged by the fourth author.

Data availability The data that supports the findings of this study are available within the article.

Declarations

Conflict of interest The authors have no conflicts to disclose.

References

1. Vlachopoulos C, O'Rourke M, Nichols W. McDonald's blood flow in arteries: theoretical, experimental and clinical principles. London: CRC Press, 2011
2. Siviglia A, Toffolon M. Steady analysis of transcritical flows in collapsible tubes with discontinuous mechanical properties: implications for arteries and veins. J Fluid Mech, 2013, **736**: 195-215
3. Isenberg B C, Williams C, Tranquillo R T. Small-diameter artificial arteries engineered in vitro. Circ Res, 2006, **98**: 25-35
4. Holzapfel G A, Gasser T C, Ogden R W. A new constitutive framework for arterial wall mechanics and a comparative study of material models. J Elast, 2000, **61**: 1-48
5. Skalak R, Keller S R, Secomb T W. Mechanics of blood flow. J Biomech Eng, 1981, **103**(2): 102-115
6. Euler L. Principia pro motu sanguinis per arterias determinando. Opera Postuma, 1862, **2**: 814-823
7. Parker H K. A brief history of arterial wave mechanics. Med Biol Eng Comput, 2009, **47**(2): 111-118
8. Montecinos G, Muller L O, Toro E F. Hyperbolic reformulation of a 1D viscoelastic blood flow model and ADER finite volumes chemes. J Comput Phys, 2014, **266**: 101-123
9. Murillo J, Montilla A V, Navarro P G. Formulation of exactly balanced solvers for blood flow in elastic vessels and their application to collapsed states. Comput Fluids, 2019, **186**: 74-98
10. Strocchi M, Contarinoa C, Zhang Q, Bonmassari R, Toro E F. A global mathematical model for the simulation of stenoses and bypass placement in the human arterial system. Appl Math Comput, 2017, **300**: 21-39
11. Ponalagusamy R, Manchi R. A study on two-layered (K.L-Newtonian) model of blood flow in an artery with six types of mild stenoses. Appl Math Comput, 2020, **367**: 124767
12. Sharma B D, Yadav P K. A two-layer mathematical model of blood flow in porous constricted blood vessels. Transp Porous Media, 2017, **120**: 239-254

13. Srivastava V P, Rastogi R, Vishnoi R. A two-layered suspension blood flow through an overlapping stenosis. Comput Math with Appl, 2010, **60**: 432-441
14. Zhang Q, Sheng W, Xiao T. Riemann problem and Godunov-type scheme for a two-layer blood flow model. Appl Math Lett, 2023, **135**: 108437
15. Ghitti B, Berthon C, Le M H, Toro E F. A fully well-balanced scheme for the 1D blood flow equations with friction source term. J Comput Phys, 2020, **420**: 109750
16. Sherwin S J, Formaggia L, Peiro J, Franke J. Computational modelling of 1D blood fow with variable mechanical properties and its application to the simulation of wave propagation in the human arterial system. Int J Numer Meth Fluids, 2003, **43**: 673-700
17. Brook B S, Falle S A E G, Pedley T J. Numerical solutions for unsteady gravity-driven flows in collapsible tubes: evolution and roll-wave instability of a steady state. J Fluid Mech, 1999, **396**: 223-256
18. Sheng W, Zhang Q, Zheng Y. The Riemann problem for a blood flow model in arteries. Commun Comput Phys, 2020, **27**: 227-250
19. Muller L O, Toro E F. Well-balanced high-order solver for blood flow in networks of vessels with variable properties. Int J Numer Method Biomed Eng, 2013, **29**(12): 1388-1411
20. Jana S, Kuila S. Riemann solutions of two-layered blood flow model in arteries. Int J of Non-Lin Mech, 2023, **156**: 104485.
21. Zhanga Q, Liu S. The Riemann problem and a Godunov-type scheme for a traffic flow model on two lanes with two velocities. Appl Math Comput, 2023, **436**: 127502
22. Aguillon N, Audusse E, Godlewski E, Parisot M. Analysis of the Riemann problem for a shallow water model with two velocities. SIAM J Math Anal, 2018, **50**: 4861-4888
23. Riemann B. Ueber die Fortpflanzung ebener Luftwellen von endlicher Schwingungsweite. Gott Abh Math Cl, 1860, **8**: 43-65
24. Lax P D. Hyperbolic systems of conservation laws II. Comm Pure Appl Math, 1957, **10**: 537-566
25. Smoller J. Shock waves and reaction-diffusion equations. New York: Springer-Verlag, 1983
26. Gupta P, Chaturvedi R K, Singh L P. The propagation of weak shock waves in non-ideal gas flow with radiation. Eur Phys J Plus, 2020, **135**: 1-15
27. Kuila S, Raja Sekhar T. Wave interactions in non-ideal isentropic magnetogasdynamics. Int J App Comp Math, 2017, **3**: 1809-1831
28. Sen A, Raja Sekhar T, Zeidan D. Stability of the Riemann solution for a 2×2 strictly hyperbolic system of conservation laws. Sadhana, 2019, **44**: 11, 8 pp.
29. Arora R, Sharma V D. Convergence of strong shock in a van der walls gas. SIAM J Appl Math, 2006, **66**: 1825-1837
30. Toro E F. Riemann solvers and numerical methods for fluid dynamics. Berlin: Springer-Verlag; 2009
31. Ambika K, Radha R. Riemann problem in non-ideal gas dynamics. Indian J Pure Appl Math, 2016, **47**(3): 501-521
32. Pandey M, Sharma V D. Interaction of a characteristic shock with a weak discontinuity in a non-ideal gas. Wave Motion, 2007, **44**: 346-354
33. Raja Sekhar T, Sharma V D. Wave interactions for the pressure gradient equations. Methods Appl Anal, 2010, **17**: 165-178
34. Minhajul, Raja Sekhar T. Nonlinear wave interactions in a macroscopic production model. Acta Math Sci, 2021, **41B**: 764-780
35. Li S, Shen C. On the wave interactions for the drift-flux equations with the Chaplygin gas. Monatsh Math, 2022, **197**: 635-654
36. von Neumann J. The theory of shock waves, in collected works. Oxford: Pergamon Press, 1963